

# Carrier Aggregation in Satellite Communications: Impact and Performance Study

Mirza Golam Kibria, Eva Lagunas, Nicola Maturo, Hayder Al-Hraishawi, and Symeon Chatzinotas

Carrier Aggregation (CA) is an integral part of current cellular networks. Its ability to enhance the peak data rate, to efficiently utilize the limited available spectrum resources and to satisfy the demand for data-hungry applications has drawn large attention from different wireless network communities. Given the benefits of CA in the terrestrial wireless environment, it is of great interest to analyze and evaluate the potential impact of CA in the satellite domain. In this paper, we provide a brief introduction to the possible CA configurations, their deployment scenarios/use cases as well as their advantages, disadvantages, and challenges. Next, the problem of multiuser aggregation and access control design for CA in multi-beam high throughput satellite systems under practical system constraints is presented. In particular, we propose an efficient CA design solution that gives the optimal carrier-user assignment along with the percentage that each user exploits each carrier assuming that multiple users can be multiplexed in each carrier. Both inter-transponder and intra-transponder CA at the satellite payload level of the communication stack are considered. We propose a flexible carrier allocation approach for a CA-enabled multi-beam satellite system targeting a proportionally fair user demand satisfaction. Simulation results and analysis shed some light on this rather unexplored scenario and demonstrate the feasibility of the CA in satellite communication systems.

**Index Terms**—High Throughput Satellite, Carrier Aggregation, Flexible Resource Allocation, Channel Bonding, Multi-beam Satellite, Dual Connectivity.

## I. INTRODUCTION

During the last decade, satellite technology has been rapidly growing due to the benefits that satellite communication systems can provide, such as ubiquitous broadband coverage over a large area, wideband transmission capability, and navigation assistance [2]. Because of these benefits, the satellite data traffic is witnessing a phenomenal growth contributed by the delivered telecommunication services in a wide range of sectors such as aeronautical, maritime, military, rescue and disaster relief [3], [4].

On the other hand, the increasing user demand for broadcast and multicast services has evidenced significant variations of the traffic requested by users in different geographical locations. The latter is leading to an escalating need for flexible satellite systems [2], where the available resources have to be dynamically assigned according to the traffic demands. In multi-beam geostationary (GEO) systems, the beam traffic unbalance can be generated by mobility customers moving across the coverage area, generating potential congestion in certain beam areas (also known as hot-spot beams).

With the ever-increasing satellite communication traffic and the rapidly growing demands for any time, and anywhere access to satellite services, the satellite spectrum resources need to be efficiently and thoroughly utilized because the system capacity significantly depends on available satellite resources and their utilization. Multiple studies have been conducted from different perspectives to enhance satellite system capacity. For instance, the works in [5], [6] propose a

joint power and bandwidth assignment for the forward link of a flexible geostationary (GEO) satellite system targeting the minimization of the unmet system capacity. Both [5], [6] rely on computationally expensive optimization techniques such as genetic algorithms and simulated annealing method. The satellite resource assignment is studied in [7], [8] also under a demand-matching approach but targeting minimization of the overall utilized resources. However, the aforementioned works consider a complete reshuffling of the user-carrier assignment with every change on the traffic demand distribution. Clearly, moving users among carriers translate into a signaling overhead and potential connectivity issues. Alternatively, [9] considers the joint optimization of essential satellite system parameters such as uplink and downlink satellite antenna gains, the ground terminals' receive gain and noise temperature, path losses and fades, and data rates to improve resource utilization.

On a parallel avenue, carrier aggregation (CA) standardized by 3rd generation partnership project (3GPP) emerged as a promising technology allowing the mobile network operators to combine multiple component carriers across the available spectrum to extend the channel bandwidth, and hence, increasing the network capabilities to respond to sudden peak data rate requests [10], [11]. When carriers are aggregated, each carrier is referred to as a component carrier. However, in this paper, we use component carrier to designate any carrier of the system. Enabling CA feature in cellular network attains significant gains in performance through exploiting the available spectrum resources and satisfying the high throughput demands [12]. Interestingly, CA does not only address the spectrum scarcity and boost peak data rate satisfaction of the users but also can maintain the system quality of service via efficient interference management and avoidance capabilities [13] when CA is combined with appropriate carrier assignment [14]. While the application of CA in terrestrial scenarios has been widely considered, its application in satellite communications is still a rather unexplored area. Recently, the application

The preliminary results of this manuscript were presented in IEEE Globecom 2019, Hawaii, USA[1]. This work has been partially supported by the Luxembourg National Research Fund (FNR) under the project FlexSAT "Resource Optimization for Next Generation of Flexible SATellite Payloads" (C19/IS/13696663) and by the ESA funded activity CADSAT: Carrier Aggregation in Satellite Communication Networks. Please note that the views of the authors of this paper do not necessarily reflect the views of ESA. The authors are with SIGCOM Research Group, SnT, University of Luxembourg. The corresponding author is Eva Lagunas (eva.lagunas@uni.lu).

of CA in the satellite communications domain has received interest from the European Space Agency (ESA), whose funded project CADSAT [15] analyzed several potential scenarios based on the market, business and technical feasibility.

Regarding the satisfaction of heterogeneous satellite user demands, CA emerges as an attractive technique with promising potential in addressing this fundamental requirement of the next generation of satellite systems. Owing to its competence in offering an additional degree of freedom on resource allocation flexibility, this paper aims to evidence the benefits due to the adoption of CA against traditional solutions.

Channel bonding as defined in DVB-S2X standard [16] is in many ways similar to the concept of CA. However, there are important differences between these two schemes. In fact, CA can be seen as an extension or improved-version of Channel Bonding (CB), as it overcomes the limitations of the CB. More precisely, CB is mainly designed for video broadcasting and designed to work only under Constant Coding and Modulation (CCM), where all the services undergo the same coding and modulation procedure, which is a very obstructive factor for its employment in the emerging broadband applications. On the other hand, Adaptive Coding and Modulation (ACM) shall be allowed in CA, such that the use of different coding schemes between aggregated channels is possible. Furthermore, CB is limited to adjacent bands, while CA referred to both contiguous and non-contiguous carriers in different spectral bands [17], [18]. Motivated by these facts, this paper focuses on CA to circumvent these limitations and improve system flexibility.

**Contributions:** We summarize the main technical contributions of this study below.

- 1) Introduce and discuss the promising and practical scenarios for deploying CA in satellite systems. In addition to elaborated descriptions and schematic diagrams of each considered CA setup, the benefits, pitfalls, and implementation complications are also highlighted.
- 2) Adopting CA techniques in satellite mobile communication systems have been investigated, and the effects of intra-transponder and inter-transponder CA at the payload level of the communication stack have been thoroughly analyzed.
- 3) An efficient multi-user aggregation scheme for CA considering user achievable capacities over different carriers has been proposed. In particular, the user-carrier association and optimal carrier fill-rate are obtained, where fill-rate indicates the percentage of bits that a particular user can utilize from a given baseband frame (of a given carrier).
- 4) The performance of the proposed CA solution has been evaluated based on its capability in minimizing the unmet and unused capacity. Simulation results are provided to confirm the efficacy of the proposed solution.

While this paper focuses on the user-carrier assignment part of CA, the authors' work in [19] presents the details on the load balancing and scheduling design at the gateway side when CA is enabled. In other words, [19] considers the user-carrier assignment as given and focuses on the link layer traffic splitting across aggregated carriers.

This paper is organized as follows. Section II provides the system model of this study. In section III, we present the multiuser aggregation and access control in the CA problem statement and the proposed solution. Section IV presents the simulation results and Section V concludes.

**Notations:** Boldface lower-case and upper-case letters define vectors and matrices, respectively.  $\mathbb{R}$  defines the real space. Superscript  $(\cdot)^T$  denotes the transpose operation and  $\text{diag}(\cdot)$  puts the diagonal elements of a matrix into a vector. Operator  $\text{vec}(\cdot)$  stacks all the elements of the argument into a vector and  $\|\cdot\|_1$  returns 1-norm of the argument.  $\mathbf{1}^{x \times y}$  defines a vector/matrix of all one elements. Similarly,  $\mathbf{0}^{x \times y}$  defines a vector/matrix of all zero elements.

## II. DEPLOYMENT SCENARIOS OF CA IN MULTIBEAM SATELLITE SYSTEM

CA in satellite systems can be differentiated based on the deployment scenarios, e.g., (i) CA in single satellite (e.g., GEO or Medium Earth Orbit (MEO)) scenarios or single-satellite CA and (ii) CA in multi-satellite scenarios or inter-satellite CA. Under the single-satellite CA, the CA will have different configurations for mono-beam and multi-beam satellites. The mono-beam CA in which multiple carriers cover the same region mainly targets load balancing between transponders to leverage underutilized spectrum and offer more bandwidth to users with high demand. On the other hand, CA in multi-beam satellite systems focuses on the poor coverage at the beam edge, and increase the peak rates of edge users assuming that one beam is congested while a neighboring beam is underutilizing its resources. Furthermore, under the inter-satellite CA mode, the combination of carriers from two or more satellites is considered. Different satellite on the same orbit and on different orbits may be considered. For instance, a multi-MEO CA considers the combination of carriers from two or more satellites in MEO orbit with overlapping beams, i.e., the user terminal belongs to the coverage of both. Another inter-satellite CA use case is the GEO-MEO CA, which combines carriers from a GEO and MEO satellite systems. A brief introduction to the possible CA scenarios is given below. The schematic descriptions of different CA scenarios is provided in Fig. 1.

- a) *Scenario-1: CA in mono-beam GEO system:* Mono-beam is usually used for broadcasting (e.g., high-definition TV (HDTV)) and it is one of the main scenarios that inspired channel bonding. With the adoption of CA under this scenario, the user links can aggregate carriers across or within transponders which might originate from the same or different Gateways (GWs). This scenario refers to the CA applied to a mono-beam multicarrier system similar to SES ASTRA [20], where multiple carriers cover the same region. This scenario targets load balancing between transponders in a single-beam case. Two transponders are assumed to cover the same region. This can be done either in Frequency Division Multiplexing (FDM) or using two polarizations (for example, horizontal and vertical polarizations) in the same bandwidth.

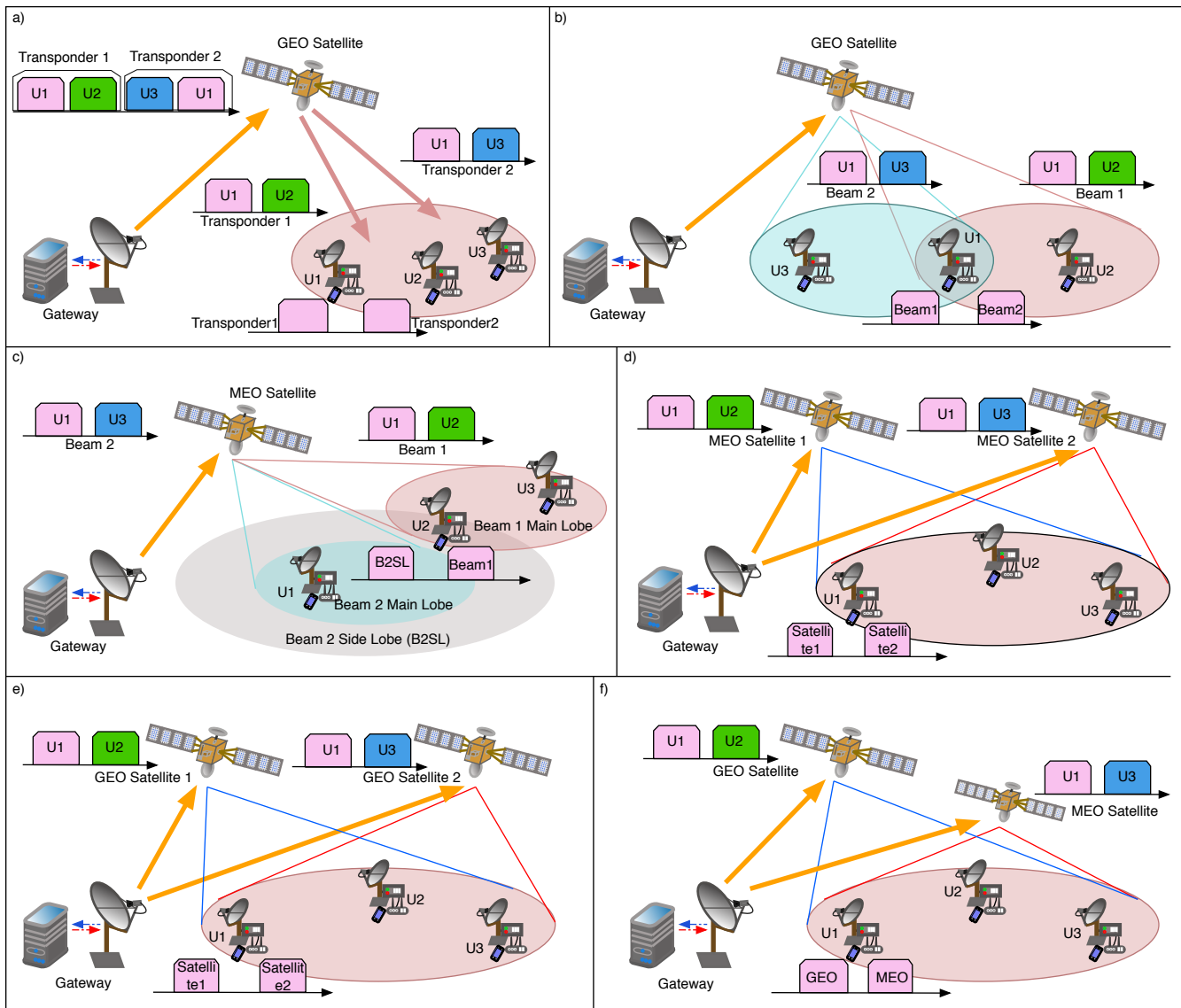


Fig. 1. Schematic descriptions of different CA scenarios: (a) Mono-beam multi-carrier GEO system, (b) Multi-beam GEO system, (c) Single MEO satellite system, (d) Aggregation across multi-MEO systems, (e) Aggregation across multi-GEO systems, (f) Aggregation across MEO and GEO systems.

- b) *Scenario-2: CA in multi-beam GEO*: CA provides flexibility to adapt to heterogeneous traffic demands, meaning the case where we have high-demand beams (aka. hot beams) and low-demand beams (aka. cold beams), by allowing the hot beams to exploit resources from cold neighboring beams which usually happens at the beam edge. This CA scenario focuses on the poor coverage at the beam edge in multi-beam High Throughput Satellite (HTS) systems. CA in this scenario can be employed to increase the peak rates of edge users. This scenario assumes that one beam is fully loaded while a neighboring beam has spare capacity. In conventional HTS, one of the main limitations is the poor coverage at the beam edge [21]. In this context, CA could be used to mitigate this problem by increasing the peak rates of edge users and providing a fairer quality of service across the coverage area. It should be noted, however, that CA would provide limited advantage when all beams

are fully loaded, as CA cannot increase the capacity of the system but rather provide a appropriate distribution of the available resources.

- c) *Scenario-3: CA in single MEO system*: This CA configuration considers the combination of carriers from multiple beams belonging to the same MEO satellite system. The aggregation may occur when beams are adjacent or via side-lobe beams. The motivation of this scenario is similar to the previous one, i.e. to enhance the service within the coverage area by balancing congested and underutilized carriers. This scenario is applicable for instance to SES O3b mPower [22]. Due to the relatively smaller size of the satellite antenna, the beam patterns exhibit significant side-lobes. This allows for aggregating transmissions from carriers over the side-lobes of adjacent beams. However, if the MEO beams are far apart, side-lobe gain may be limited, thereby limiting the applicability of this particular use case.

- d) *Scenario-4: CA across multi-MEO systems*: This scenario focuses on combining carriers from 2 or more satellites in MEO orbit. This solution can provide increased peak rates for hot-spots by using adjacent cold (with less demand/unused capacity) satellites. The cold satellite carrier could go through the side lobe in case no available antennas can be pointed directly to the aggregating user terminal. This scenario differs from scenario 3 both in architecture (multiple vs single satellite) as well as the aim (high rate vs. min rate provisioning). This scenario is particularly interesting for aeronautical and maritime service. In order to get significant gains, the coverage of the aggregated MEO systems need to overlap so that sufficient signal power is received from both satellites. Furthermore, due to the satellite movement, the propagation distance will change at any second. This will cause dynamic imbalance and possibly constant changes which put some challenges into the load balancing module [19].
- e) *Scenario-5: CA across multi-GEO systems*: The CA configuration considers the combination of carriers from two or more satellites in a GEO orbit. Multiple satellites can improve the rate when bringing in multiplexing gain, however as rain fading is close to the users, unless the satellite orbital slots are very far apart, it is not clear if significant gains can be achieved. Furthermore, if aggregation happens over different orbital slots, two different antenna dishes need to be considered at the terminal side. All in all, GEO-GEO link aggregation is foreseen to be marginally useful in very specific use cases.
- f) *Scenario-6: CA across different orbits*: Scenario 6 combines carriers from satellite systems in different orbits, e.g. MEO and GEO. This is a challenging scenario, where one or multiple satellites are in movement. The different delay between the two systems is the major issue. In addition, complex user terminals are foreseen for this scenario involving different dishes. This scenario is therefore considered as only applicable to certain cases such as military ships, remote areas, etc. The advantage can be for example in backhauling, where one carrier is fixed on GEO and another one tracks MEO and aggregated the two links in one.

Note that different CA configurations come up with some inherent advantages and disadvantages over each other. The complexity (at gateway and user terminal level) of implementation of different CA scenarios also varies. The business impact from the satellite operator perspective is also an important aspect for the success of CA in satellite systems. Therefore, the selection of the best CA scenario in the satellite domain is not straight-forward, and it is out of the scope of this study. Furthermore, devising a generalized CA framework that covers all the possible single- and multiple-satellite scenarios may not be practical from implementation point of view as some CA scenarios are quite different to other scenarios, for example, single-satellite and multiple-satellite CA scenarios. For some scenario, the system may have both static and moving beams, i.e., the multi-satellite GEO/MEO scenario.

Therefore, a generalized CA framework is inefficient as different scenarios will have different sets of constraints based on the architecture(s). Also, a generalized CA framework will not be able to capture the inherent characteristics of all individual scenarios. Scenario-1 and Scenario-2 seem to be two promising CA scenarios in satellite communications. Since both the scenarios can be captured by Scenario-2 and Scenario-2 appears to provide a good performance-complexity trade-off, we consider this scenario as a baseline for our study.

### III. MULTIUSER ACCESS CONTROL FOR CA IN SATELLITE SYSTEMS

#### A. CA overall architecture

A multi-beam GEO satellite system that employs multi-carrier transponders is considered. In particular, we focus on the aforementioned *Scenario-2: CA in multi-beam GEO*, where both intra-transponder and inter-transponder CA can take place. Let the total number of users in the system be  $N_U$  while the total number of carriers is  $N_C$ . Each carrier has a bandwidth of  $B_w$  MHz. A fixed number of carriers across beams is assumed. However, the number of component carriers may vary across beams. The carriers may be shared with multiple users. A schematic model example of the considered system is given in Fig. 2, where the satellite has five multi-carrier transponders each with two carriers.

In our considered system model, the carrier assignment is dynamic based on user traffic demand. Based on the user demand and link budget per carrier, the user-carrier association is determined along with the fill-rates. Instead of allowing the users to be constantly logged-on in a single carrier (as in conventional satellite systems), we rather consider that the carriers are dynamically enabled to premium terminals whenever needed, allowing users to simultaneously operate in  $\leq \Delta_{\max}$  carriers. However, this model implies more complexity in terms of user traffic monitoring and reconfigurable capabilities of the system.

CA essentially duplicates the Medium Access Control (MAC) and Physical (PHY) layer processing for each component carrier while keeping radio-link control (RLC) and above identical to the non-aggregation case. In particular, the Radio Link Control (RLC) layer provides the logical channels, and if the carrier aggregation is enabled, the MAC layer functionality will then split the data on multiple downlink carriers, as illustrated in Fig. 2. More precisely, the load balancing and Packet Data Unit (PDU) scheduler takes the single data stream and splits the traffic across the aggregated carriers. Then, the Generic Stream Encapsulation (GSE) blocks take the corresponding PDUs and generates different GSE packets, which are subsequently scheduled in the baseband frames (BBFRAMES). From the CA blocks shown in Fig. 2, this paper focuses on the Multiuser Aggregation and Access Control (MAAC) block design. Details on the Load Balancing and Scheduler block design are provided in [19].

#### B. MAAC Design

This section first introduces the optimization variables and key parameters that are employed on the definition of the



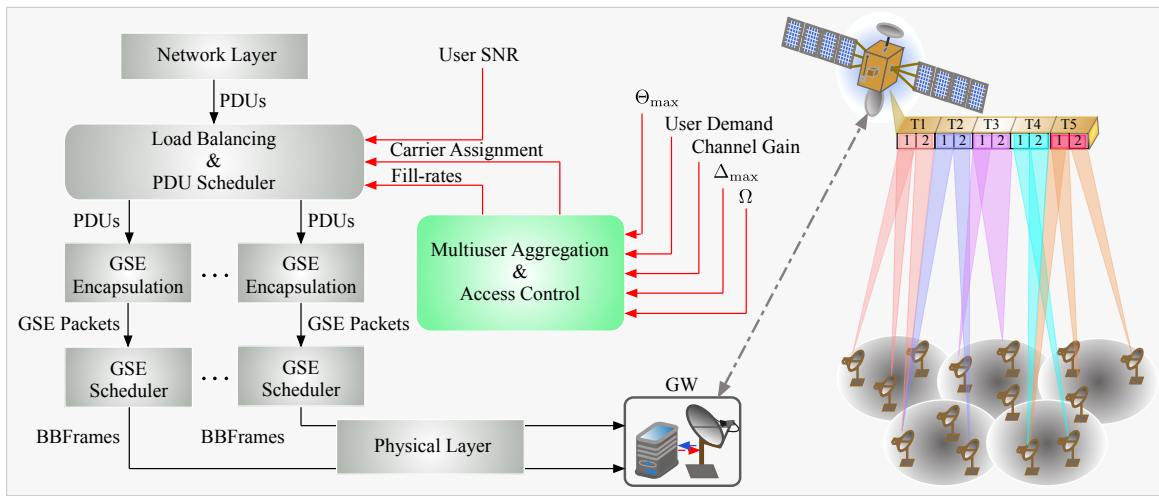


Fig. 2. Schematic model of the CA. In this example, there are 5 multicarrier transponders, namely  $T_1, T_2, \dots, T_5$ , each with 2 component carriers. There can be inter-transponder CA as seen in  $T_1$  and  $T_2$  where user of  $T_2$  is served by carriers of  $T_1$  and  $T_2$  as well as intra-transponder CA as seen in  $T_3$  where both carriers served one of its users.

MAAC design problem statement. Next, the design constraints are provided based on the defined parameters.

Description of the main involved variables are provided below:

- Carrier-User Binary Assignment Variable ( $a_{c,u}$ ): If carrier  $c$  is assigned to user  $u$ , then  $a_{c,u} = 1$ , otherwise  $a_{c,u} = 0$ .
- Fill-rate variable ( $f_{c,u}$ ): Carrier may be shared by multiple users. The fill-rate of a given user  $u$  for a given carrier  $c$  is defined as the fraction of that carrier's bandwidth assigned to the given user. The fill-rate can also be seen as the percentage of time that user  $u$  utilizes the baseband frame of carrier  $c$  on an average during the service period. The value of  $f_{c,u}$  lies between 0 and 1. If carrier  $c$  is used in full by user  $u$ ,  $f_{c,u} = 1$ . Likewise, if carrier  $c$  is used in part by user  $u$ , then  $0 < f_{c,u} < 1$ . If carrier  $c$  is not used by user  $u$ , then  $f_{c,u} = 0$ .
- Achievable rate ( $r_{c,u}$ ): This indicates the data rate that is achieved by user  $u$  when this operated only in carrier  $c$  with  $f_{c,u} = 1$ . The value of  $r_{c,u}$  is assumed to be perfectly know in this work, as it can be obtained based on the channel-state information and link budget. In particular,

$$r_{c,u} = B_w [f_{SE}(\text{CINR}_{c,u})], \quad (1)$$

where  $\text{CINR}_{c,u}$  denotes the Carrier-to-Interference plus Noise Ratio (CINR) for user  $u$  at carrier  $c$ . The function  $f_{SE}$  maps the CINR value to appropriate spectral efficiency according to the Adaptive Coding and Modulation (ACM) schemes proposed in the DVB-S2(X) standard.

Next, the design of the MAAC block is formulated under a demand-matching fairness criteria. First, let us define the overall offered capacity to user  $u$  as,

$$s_u = \sum_{c=1}^{N_C} f_{c,u} r_{c,u}. \quad (2)$$

The objective of the MAAC design is to satisfy the user traffic demands, denoted as  $d_u$ ,  $u = 1, \dots, N_U$ , in a fair

manner. In particular, we opt to maximize the minimum of  $\frac{s_u}{d_u}$ ,  $u = 1, 2, \dots, N_U$ . Therefore, the objective of the considered MAAC design is given by,

$$\max_{a_{c,u}, f_{c,u}} \min_{u=1, \dots, N_U} \frac{s_u}{d_u}. \quad (3)$$

In the following, we list the constraints that apply to the MAAC design:

- The maximum number of carriers that can be aggregated by a single premium user shall be upper-bounded based on the user terminal chip-set architecture. We can mathematically express this constraint as follows,

$$\sum_{c=1}^{N_C} a_{c,u} \leq \Delta_{\max}, u = 1, 2, \dots, N_U \quad (4)$$

where  $\Delta_{\max}$  is the maximum number of parallel streams, i.e., carriers that the user terminal can aggregate simultaneously.

- The summation of bandwidths used by different users operating on the same carrier must not exceed the carrier bandwidth. For a carrier with bandwidth  $B_W$ , this is formulated as  $\sum_{u=1}^{N_U} f_{c,u} B_W \leq B_W$ . Therefore, this constraint can be expressed as,

$$\sum_{u=1}^{N_U} f_{c,u} \leq 1, c = 1, 2, \dots, N_C \quad (5)$$

- Ideally, we would like the user-carrier assignment to adapt to the dynamic variations of the demand with the minimal amount of carrier swapping to reduce the signaling overhead and link outage/degradation. Let us assume a system running with a given carrier assignment at time-instant  $t$ , which has been obtained based on a particular user traffic demand instance. At  $t + 1$ , the user demands change, and the user-carrier assignment needs to be updated accordingly. For instance, some high demand users at  $t$  may request lower demand capacity at  $t + 1$ , while some low demand users at  $t$  may now

request higher demand capacity at  $t+1$ . Some users may just go off while some new users may become active. Under such demand change circumstances, the MAAC unit needs to reconfigure the user-carrier association as well as the fill-rates. Ideally, we would prefer to move as fewer users as possible to minimize signaling overhead and link outage/degradation during the carrier swapping. Therefore, as demand changes, the user-carrier association and fill-rates need to be re-designed such that the difference from the previous state is minimized. The latter is mathematically formulated as,

$$\|\text{vec}(\mathbf{A}(t+1)) - \text{vec}(\mathbf{A}(t))\|_1 \leq \Omega \quad (6)$$

where  $\Omega$  is the maximum number of changes allowed in the subsequent carrier assignment, and  $\|\mathbf{x}\|_1 = \sum_{r=1}^n |x_r|$  is the  $L^1$ -norm of vector  $\mathbf{x} = [x_1, x_2, \dots, x_n]$ . Here,  $\mathbf{A}$  is defined as the carrier assignment matrix, i.e., a binary matrix of size  $N_C \times N_U$  with  $(i, j)$ -th element of  $\mathbf{A}$ ,  $\mathbf{A}_{i,j} = a_{i,j}$ .  $\mathbf{A}(t)$  denotes the carrier assignment matrix at time-instant  $t$ .

- In general, from the complexity point of view, it is preferable to aggregate few carriers with high fill-rate rather than many carriers with small fill-rate. In addition, if the aggregation of a particular carrier does not bring much gain, it may not be worth to perform the aggregation. As a consequence, the MAAC unit should avoid aggregating carriers whose gain or throughput is marginal. For example, for a CA user with two carriers with equal bandwidth, the fill-rate over one carrier can be very small compared to the fill-rate over the second carrier. Intuitively, the users with high demand are expected to perform carrier aggregation, and when there is carrier aggregation for a given user, the fractions of individual fill-rates compared to the overall sum-of fill-rates should be above some given threshold. In other words,

$$\frac{f_{c,u}}{\sum_{c=1}^{N_C} f_{c,u}} \geq \Theta_{\max}, \quad u = 1, 2, \dots, N_U \quad (7)$$

where  $0 < \Theta_{\max} \leq 1$  defines the measure of balance between different fill-rates or the threshold. From the constraint in (7), it is clear that for a CA user, the maximum value of  $\Theta_{\max}$  can be as high as 1/2 when two carriers are aggregated and 1/3 when three carriers are aggregated.

### C. MAAC Design Problem Statement

Based on our system model and the constraints already discussed, the problem can be expressed as follows,

$$\begin{aligned} & \max_{a_{c,u}, f_{c,u}} \min_{u=1, \dots, N_U} \frac{s_u}{d_u} \\ & \text{subject to} \quad \text{C1: } \sum_{c=1}^{N_C} a_{c,u} \leq \Delta_{\max}, u = 1, 2, \dots, N_U, \\ & \quad \text{C2: } \sum_{u=1}^{N_U} f_{c,u} \leq 1, c = 1, 2, \dots, N_C, \\ & \quad \text{C3: } \|\text{vec}(\mathbf{A}(t+1)) - \text{vec}(\mathbf{A}(t))\|_1 \leq \Omega \\ & \quad \text{C4: } \frac{f_{c,u}}{\sum_{c=1}^{N_C} f_{c,u}} \geq \Theta_{\max}, u = 1, 2, \dots, N_U \\ & \quad \text{C5: } a_{c,u} \in \{0, 1\}, u = 1, \dots, N_U, c = 1, \dots, N_C \\ & \quad \text{C6: } 0 \leq f_{c,u} \leq 1, u = 1, \dots, N_U, c = 1, \dots, N_C \end{aligned} \quad (8)$$

Note that the constraints in the considered problem statement (8) do not deliver the expected mapping between the association indicator  $a_{c,u}$  and the fill-rate variable  $f_{c,u}$ . In particular, if the output  $f_{c,u} > 0$ , the value of  $a_{c,u}$  shall be 1, and if  $f_{c,u} = 0$ , then  $a_{c,u}$  shall be 0. To deal with this issue, we introduce the following *conditional* constraints to the existing problem statement and replacing it with C4 in (8).

$$\text{C4: } \begin{cases} \text{N1: } f_{c,u} = 0 \text{ IF } a_{c,u} = 0 \\ \text{N2: } f_{c,u} \geq \Theta_{\max} \sum_{c=1}^{N_C} f_{c,u} \text{ IF } a_{c,u} = 1 \end{cases} \quad (9)$$

Consequently, the refined problem statement can now be expressed as,

$$\begin{aligned} & \max_{a_{c,u}, f_{c,u}} \min_{u=1, \dots, N_U} \frac{s_u}{d_u} \\ & \text{subject to} \quad \text{C1: } \sum_{c=1}^{N_C} a_{c,u} \leq \Delta_{\max}, u = 1, 2, \dots, N_U, \\ & \quad \text{C2: } \sum_{u=1}^{N_U} f_{c,u} \leq 1, c = 1, 2, \dots, N_C, \\ & \quad \text{C3: } \|\text{vec}(\mathbf{A}(t+1)) - \text{vec}(\mathbf{A}(t))\|_1 \leq \Omega \\ & \quad \text{C4: } \begin{cases} \text{N1: } f_{c,u} = 0 \text{ IF } a_{c,u} = 0 \\ \text{N2: } f_{c,u} \geq \Theta_{\max} \sum_{c=1}^{N_C} f_{c,u} \text{ IF } a_{c,u} = 1 \end{cases} \\ & \quad \text{C5: } a_{c,u} \in \{0, 1\}, u = 1, \dots, N_U, c = 1, \dots, N_C \\ & \quad \text{C6: } 0 \leq f_{c,u} \leq 1, u = 1, \dots, N_U, c = 1, \dots, N_C \end{aligned} \quad (10)$$

The optimization problem in (10) is a mixed integer nonlinear programming problem since the *conditional* constraint in C4 is nonlinear and the presence of both binary integer ( $a_{c,u}$ ) and continuous variable ( $f_{c,u}$ ). In the following, a convex mixed-integer linear programming problem is proposed which can be solved efficiently.

## IV. PROPOSED SOLUTION

In this section, an efficient formulation of the MAAC design problem is introduced for efficient CA operation in multi-beam satellite systems.

Note that  $s_u$  is an affine function of  $f_{c,u}$ , and so is  $\frac{s_u}{d_u}$ . Therefore,  $\min_{u=1, \dots, N_U} \frac{s_u}{d_u}$  is concave, and maximizing the min is convex. Hence, the objective in its current form is convex. The optimization problem in (10) is equivalent to choosing  $\{a_{c,u}, f_{c,u}, \psi\}$  to maximize  $\psi$  subject to an additional constraint  $\frac{s_u}{d_u} \geq \psi, \forall u \in \{1, 2, \dots, N_U\}$ . The latter can be expressed as,

$$\begin{aligned} & \max_{a_{c,u}, f_{c,u}, \psi} \psi \\ & \text{subject to} \quad \text{C7: } s_u \geq \psi d_u, u = 1, 2, \dots, N_U \end{aligned} \quad (11)$$

Again, since the  $\frac{s_u}{d_u}$  functions are concave over  $f_{c,u}$ , maximization of  $\psi$  is a convex optimization problem. Maximization with either the objective in (10) or with its equivalent form (11) will yield a solution that provides an offered capacity proportional to the different user traffic requests in a fairness manner. Therefore, we will obtain  $s_1 : s_2 : \dots : s_{N_U} \approx d_1 : d_2 : \dots : d_{N_U}$ , i.e., the higher the demand, the higher the offered capacity.

Note that the *conditional* constraint C4 in (10) is nonlinear. The following linear constraints will linearize the nonlinear *conditional* constraint.

$$C4 : \begin{cases} L1 : f_{c,u} \leq a_{c,u} \\ L2 : f_{c,u} \geq \Theta_{\max} \sum_{c=1}^{N_C} f_{c,u} - (1 - a_{c,u}) \end{cases} \quad (12)$$

So if  $a_{c,u} = 0$ , then  $f_{c,u}$  is 0 by the first constraint L1 (while L2 has no effect). On the other hand, if  $a_{c,u} = 1$ , L1 has no impact while L2 prevails. Thus, (12) ensures the expected mapping between the association indicator  $a_{c,u}$  and the fill-rate variable  $f_{c,u}$ .

Incorporating (12) to (11), we obtain the following problem statement,

$$\begin{aligned} & \max_{a_{c,u}, f_{c,u}, \psi} \psi \\ & \text{subject to} \quad C1: \sum_{c=1}^{N_C} a_{c,u} \leq \Delta_{\max}, u = 1, 2, \dots, N_U, \\ & \quad C2: \sum_{u=1}^{N_U} f_{c,u} \leq 1, c = 1, 2, \dots, N_C, \\ & \quad C3: \|\text{vec}(\mathbf{A}(t+1)) - \text{vec}(\mathbf{A}(t))\|_1 \leq \Omega \\ & \quad C4: \begin{cases} L1 : f_{c,u} \leq a_{c,u} \\ L2 : f_{c,u} \geq \Theta_{\max} \sum_{c=1}^{N_C} f_{c,u} - (1 - a_{c,u}) \end{cases} \\ & \quad C5: a_{c,u} \in \{0, 1\}, u = 1, \dots, N_U, c = 1, \dots, N_C \\ & \quad C6: 0 \leq f_{c,u} \leq 1, u = 1, \dots, N_U, c = 1, \dots, N_C \\ & \quad C7: s_u \geq \psi d_u, u = 1, 2, \dots, N_U \end{aligned} \quad (13)$$

As mentioned earlier, for the MAAC module with  $\Delta_{\max} = 2$ , the highest value  $\Theta_{\max}$  can reasonably take is 0.50. If we set the value of  $\Theta_{\max}$  to be higher than 0.50, the MAAC module in (13) will not allow CA, i.e., all the users will be assigned with just one carrier. Thus we expect lower offered capacity as well as degraded fairness index if  $\Theta_{\max}$  is set to higher than 0.50.

The optimization problem in (13) is a mixed-integer linear programming problem and can be efficiently solved with standard optimization toolbox like CVX [23].

To evaluate the fairness of the proposed solution, we make use of the Jain's Fairness Index proposed in [24]. In this paper, we use the Jain's fairness metric as a measure of how the provided rate matches the demand at a user level. For this, we define  $\zeta_u$  as the ratio between the offered capacity  $s_u$  and the demanded/ideal capacity  $d_u$ , i.e.,  $\zeta_u = \frac{s_u}{d_u}$ . In this context, the Jain's fairness index is defined as,

$$J_{FI} = \frac{\left(\sum_{u=1}^{N_U} \zeta_u\right)^2}{N_U \sum_{u=1}^{N_U} \zeta_u^2}. \quad (14)$$

A totally fair MAAC design will yield  $J_{FI} = 1$  with  $\zeta_1 = \zeta_2 = \dots = \zeta_{N_U}$ . As the disparity increases, the fairness decreases. The  $J_{FI}$  is bounded between  $1/N_U$  and 1.

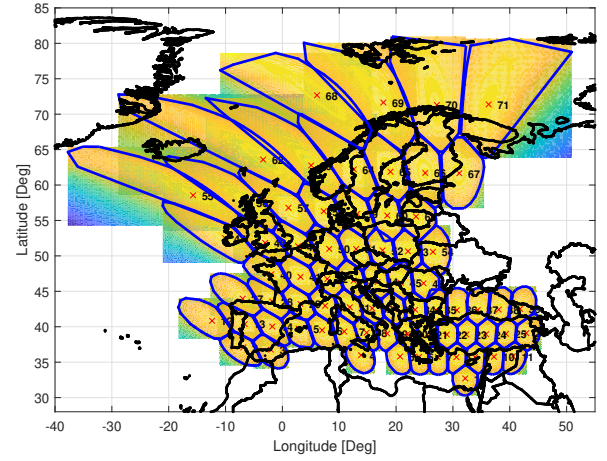


Fig. 3. ESA71 beam pattern

## V. SIMULATION RESULTS

The simulation set-up for evaluating the performance of CA in a high throughput satellite system is as follows. A 71-beam GEO satellite beam pattern provided by ESA is considered (depicted in Fig. 3). In this framework, we extract a cluster of 2,4 or 8 adjacent beams from the total pattern for different simulation scenarios. The carrier bandwidth is 54 MHz. The transmit power per beam is set to 12.24 Watt. The simulation parameters are provided in Table I. The proposed CA scheme is evaluated by quantifying peak and the average rate of the users to assess the gains concerning the system without CA. The results presented in this section have been obtained with the MATLAB-based software tool developed within the context of ESA CADSAT project [25].

TABLE I  
SIMULATION PARAMETERS

Satellite longitude	13°E (GEO)
Number of carriers per beam	2
Transmit power per beam, $P_T$	12.24 W
Number of beams, $N_B$	2,4,8
Beam radiation pattern	Provided by ESA
Downlink carrier frequency	19.5 GHz
Carrier bandwidth, $B_W$	54 MHz
Maximum number of decoded carriers, $\Delta_{\max}$	4

Regarding the generation of the users' demands,  $d_u$ ,  $u = 1, \dots, N_U$ , we consider the overall average capacity of the system  $\bar{C}$ . The latter can be obtained as an average over all the user present in the system of the supplied capacity when all resources are devoted to a single user. Two types of users are considered, namely high-demand users (or premium users) and non-high demand users. In this paper, it is assumed that the demand of a high-demand user is 20 times higher than the demand of a non-high demand users, i.e.  $\bar{d}_{HD} = 20\bar{d}_{NHD}$ . Denoting  $N_{HD}$  and  $N_{NHD}$  as the number of high-demand and non-high demand users, respectively, the average demand of non-high demand users is obtained as,

$$\bar{d}_{NHD} = \frac{\bar{C}}{20N_{HD} + N_{NHD}}. \quad (15)$$

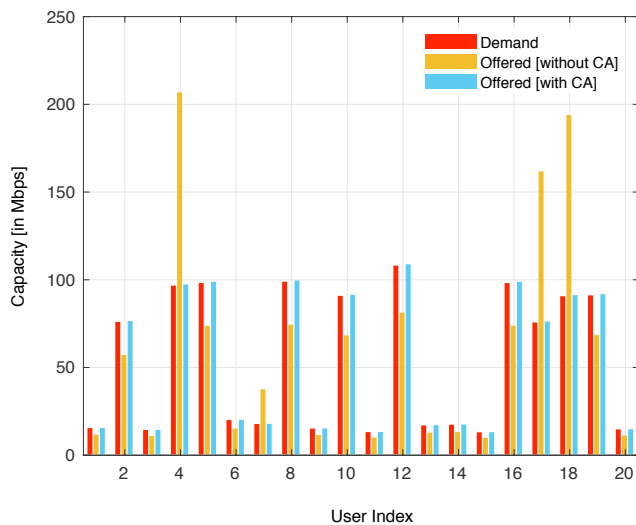


Fig. 4. Achievable offered capacity with and without CA.  $N_B = 2$ ,  $N_C = 4$  (2 per beam),  $N_U = 20$ ,  $\Delta_{\max} = 4$ ,  $\Theta_{\max} = 0.20$ .

To generate different demand instances per users, in this paper we opt for a uniformly random distribution between  $[\bar{d}_x - \Delta_x, \bar{d}_x + \Delta_x]$ , where  $x$  is used here to denote the type of users  $x \in \{HD, NHD\}$ , and  $\Delta_x$  denotes the allowed deviation from the mean. In [25],  $\Delta_x$  was set to  $\bar{d}_x/4$ . Unless otherwise stated,  $N_{HD} = N_{NHD}$ .

One of the widely used figures of merits for resource allocation in satellite communications is the unmet capacity, which is the total amount of demanded capacity that cannot be satisfied with the available resources. The unmet capacity is defined as  $C_{\text{unmet}} = \sum_{u=1}^{N_U} (d_u - s_u)^+$ , where  $(x)^+ = \max(0, x)$ . Similarly, unused capacity is another common figure of merit that corresponds to the sum of offered capacity across the beams which exceeds the demanded capacity, which is defined as  $C_{\text{unused}} = \sum_{u=1}^{N_U} (s_u - d_u)^+$ . The  $C_{\text{unmet}}$  and  $C_{\text{unused}}$  values deliver evidence of the efficiency of the proposed CA solution.

In Fig. 4, the performance of the proposed CA solution is evaluated in terms of its capability in enhancing the peak data rate of the high demand users as well as in rate-matching. In particular, a system with 2 beams with 2 component carriers per beam and 20 users is considered. The values of  $\Delta_{\max}$  and  $\Theta_{\max}$  are set to 4 and 0.2, respectively. A hot-cold beam scenario is considered, where one of the beams has very high demand (higher than the beam's average capacity) while the other beam has lower demand (lower than the beam's average capacity). The hot-cold beam scenario is generated by distributing  $> 50\%$  in the geographical coverage of one of the beams. Without CA, certain users belonging to the hot-beam do not receive enough supplied capacity to satisfy their demand. Most important, without CA, the hot-beam cannot exploit the underutilized resources of the cold beam. On the other hand, the proposed solution for CA not only is able to offer the requested capacity but also opts to treat all the users as fairly as possible. With CA, the hot beam can utilize the resources of the cold beam to serve its users.

The overall system unmet and unused capacity is evaluated

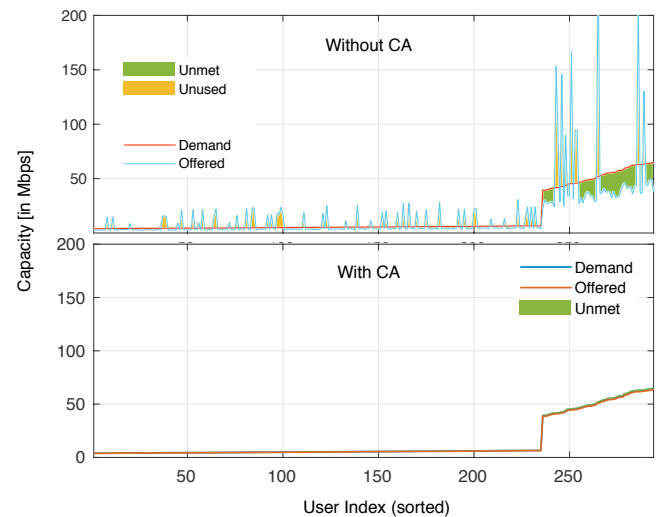


Fig. 5. Unmet vs. unused capacity comparison between satellite systems without CA (top) and with CA (bottom). The users are sorted based on their demands.

in Fig. 5 for systems with and without CA. A system with 8 beams (4 beams are configured as cold beams while the remaining beams are configured as hot beams) with 2 component carriers each and 294 users is considered for this experiment. 30% of users are high demand users while 70% of the users are in the hot beams. The values of  $\Delta_{\max}$  and  $\Theta_{\max}$  are set to 4 and 0.20, respectively. Fig. 5-top shows the unused and unmet capacity without CA and rate-matching while Fig. 5-bottom depicts the performance with CA along with our proposed rate-matching solution. It is evident from the comparisons in Fig. 5 that the proposed CA solution performs exceptionally well in utilizing the satellite resources, i.e., in reducing the unmet and unused capacity. In this current evaluation, the total demand in the system is 4.291 Gbps. The unmet and unused capacity without CA is 1.157 Gbps and 1.609 Gbps, respectively. On the other hand, the unmet and unused capacity with CA is 78 Mbps and 0 Mbps, respectively. Note that in the case of the system without CA, the available satellite capacity was assigned proportionally among the users based on their demand. As the objective of our proposed MAAC for CA is to maximize the rate matching, the total offered with the proposed CA is lower than that without CA. However, the amount of unmet and unused capacity with the proposed solution is much smaller than that without CA. Without CA, the unused capacity is higher for the low demand users while the high demand users have a relatively higher unmet capacity. While with CA, the unused/unmet capacity remains very low for all the users.

Next, the evolution of useful supply, unmet and unused capacity is evaluated in Fig. 6 for an increasing overall system demand. The system considers 2 beams with 2 component carriers per beam and a total of 25 users. The values of  $\Delta_{\max}$  and  $\Theta_{\max}$  are set to 4 and 0.2, respectively. The different demand instances are generated scaling up and down the ratio of the number of high demand users to the number of low demand users. It can be seen that for overall lower



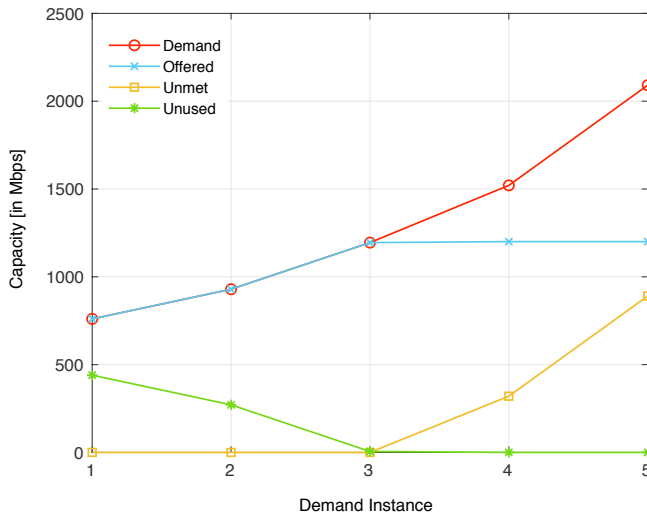


Fig. 6. Relation among the demand, supply, unmet and unused capacities.  $N_B = 2$ ,  $N_C = 4$  (2 per beam),  $N_U = 25$ ,  $\Delta_{\max} = 4$ ,  $\Theta_{\max} = 0.20$ .

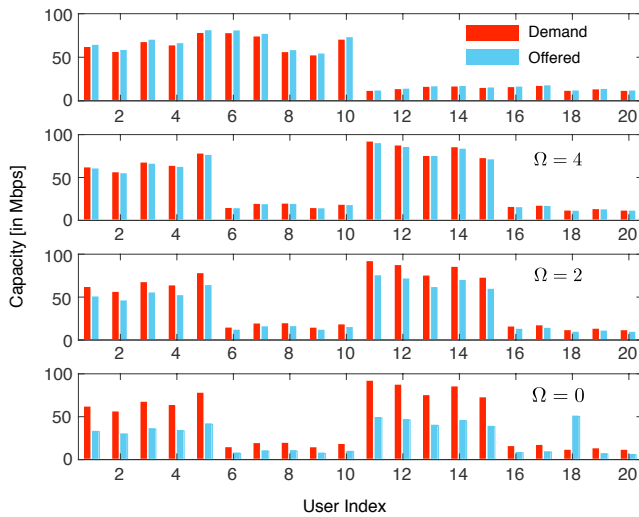


Fig. 7. Impact of values of  $\Omega$  on achievable capacity and rate matching characteristics as well as on unmet and unused capacities.  $N_B = 2$ ,  $N_C = 4$  (2 per beam),  $N_U = 20$ ,  $\Theta_{\max} = 0.20$ .

demand as compared to the average offered capacity, the users' demands can be easily satisfied, however, it gives rise to unused capacity. As the demand increases, the offered capacity keeps increasing until it reaches up to the level of average offered capacity of the system. For demands higher than what the system can offer, the useful offered capacity remains the same. On the other hand, as demand increases, the unused capacity keeps decreasing, and at one point it goes down to zero and remains the same. However, when the demand goes above what the system can deliver on an average, the satellite system has the unmet capacity, and it keeps increasing as the demand increases.

Next, we study the impact of the constraint C3 in limiting the number of user-carrier changes in response to a demand change. In Fig. 7, we show how the proposed CA solution reacts to changes in user demands depending on different values of  $\Omega$  in C3 of (13) considering two different demand

profiles. A system of 2 beams and 20 users is considered. Subplot-1 (on top) belongs to demand profile 1 and the remaining subplots 2 to 4 (below subplot-1) in Fig. 7 belong to demand profile 2. Under demand profile 1, users indexed with 1 to 10 are high demand users while the remaining users have lower demands. Under demand profile 2, some of the high demand users (indexed with 5 to 10 in demand profile 1) become low demand users while some low demand users (indexed with 11 to 15 in demand profile 1) become high demand users. Therefore, demand profile 2 (demand at time instant  $t + 1$ ) can be treated as the time evolution of demand profile 1 (demand at time instant  $t$ ). It can be observed that, when the demand changes and the value of  $\Omega$  is low, the resulting demand-offered matching is poor. However, when we relax the constraint with higher values of  $\Omega$ , the rate-matching performance improves. Hence, the subplot corresponding to  $\Omega = 4$  in Fig. 7 exhibits the best rate-matching along with smaller unmet and unused capacity. Therefore, the unmet and unused capacity gradually improves, i.e., become smaller as we increase the values of  $\Omega$ . However, as we mentioned earlier, the value of  $\Omega$  needs to be traded-off with respect to the tolerable signaling overhead resulting from multiple carrier swapping.

In the following, we study in more detail the number of aggregated carriers per user under different scenarios. In particular, Fig. 8 shows results for a system with 2, 4 and 8 beam system and considering 100 different demand realizations. Fig. 8a depicts the number of users that are carrier-aggregated with at least 2 carriers in three different system configurations. The straight lines define the average number of CA users. It can be observed that the number of CA users fluctuates marginally for a smaller system while the number fluctuates greatly as the dimension of the system increases. The only reason for that is that the bigger the cluster the more intra-/inter-beam CA occurs, as the ratio of the number of users with a higher demand to the number of users with lower demand is the same in all the systems with the varying number of beams.

Fig. 8b shows the maximum number of aggregated carriers per user. From Fig. 8b, it is evident that the users rarely aggregate 4 carriers (even when they are allowed to). For the system with 2 beams and 30 users, most of the time, the maximum number of carriers aggregated by a CA is 2. There are very few demand realizations where the maximum number of carriers aggregated is 3. As the number of beams and users increase, the frequency of aggregating 3 carriers increases. For a system with 8 beams and 120 users, there are only 2 demand realizations out of 100 when a maximum of 4 carriers are aggregated. Finally, Fig. 8c presents the number of CA users that aggregate the maximum number of carriers. It can be observed that, for the system with 2 beams and 30 users, the number of users performing carrier aggregation with 3 carriers is 1 in all the demand realizations with the maximum number of carriers aggregated equal to 3. For the system with 4 beams and 60 users, the number of users performing carrier aggregation with 3 carriers is 1 to 2 in all the demand realizations with the maximum number of carriers aggregated equal to 3. On the other hand, for the system with 8 beams and 120 users, the number of users performing carrier aggregation

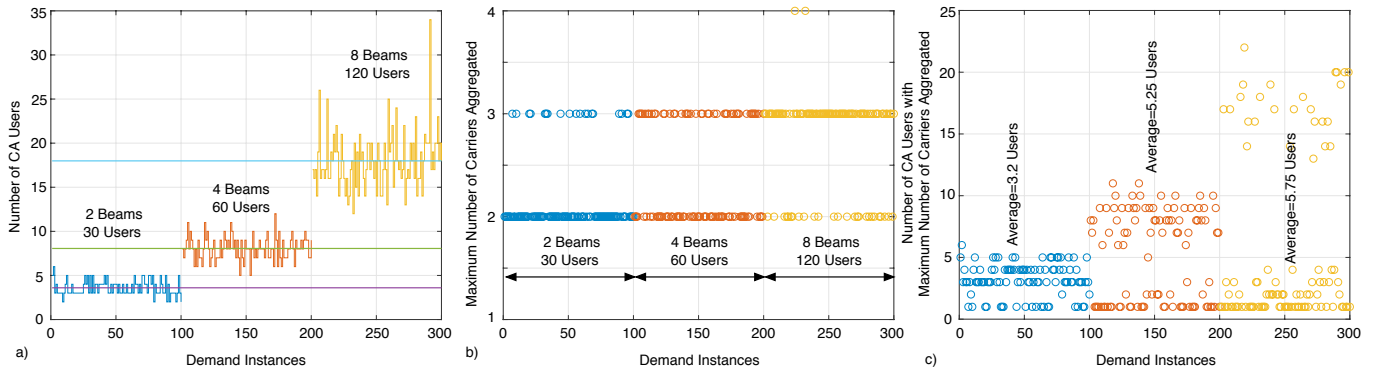


Fig. 8. a) Number of CA users over different demand instances/realizations, b) Maximum number of component carriers aggregated by a CA user, and c) Number of users with maximum number of component carriers aggregated by a CA user. A value of  $\Theta_{\max} = 0.20$  is assumed

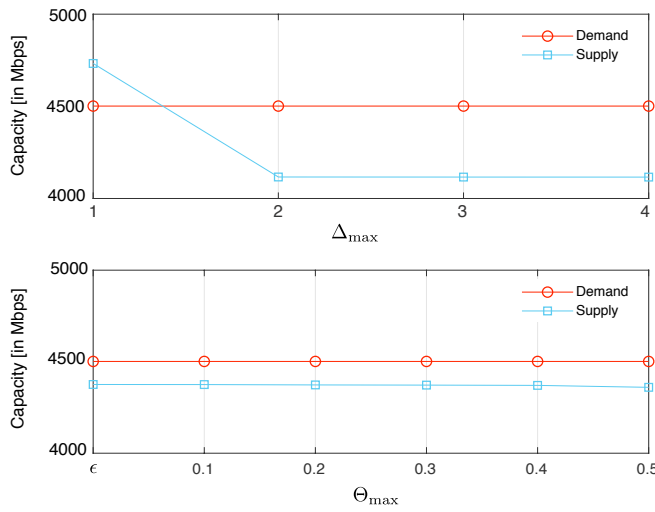


Fig. 9. top:  $\Delta_{\max}$  versus total offered capacity, and bottom:  $\Theta_{\max}$  versus total offered capacity. The system parameters are:  $N_B = 8$ ,  $N_C = 16$  (2 carriers per beam),  $N_U = 120$ .

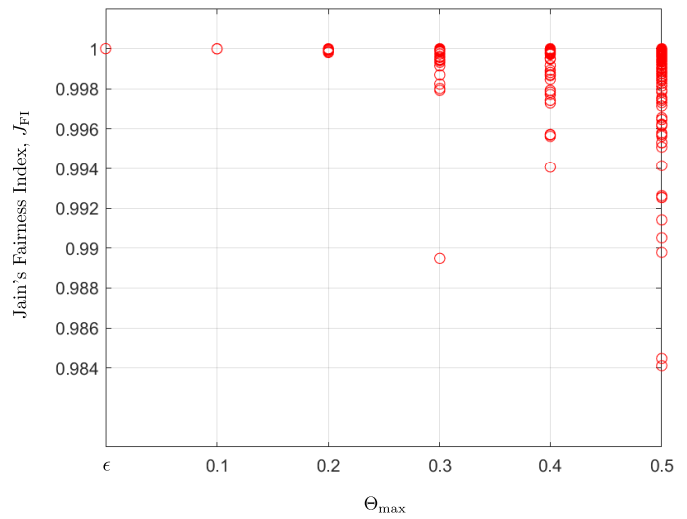


Fig. 10. Jain's fairness Index of the proposed MAAC design.  $N_B = 2$ ,  $N_C = 4$  (2 per beam),  $N_U = 25$ ,  $\Delta_{\max} = 4$ .

with 3 carriers is 1 to 5 in all the demand realizations with maximum number of carriers aggregated equal to 3, and the number of users performing carrier aggregation with 4 carriers is 1 in all the demand realizations (only 2 realization as seen in Fig. 8b) with maximum number of carriers aggregated equal to 4. Therefore, the average numbers quantified in Fig. 8c mainly corresponds to aggregation of 2 carriers for the system with 2 beams and 3 carriers for the system with 4/8 beams.

In Fig. 9, we analyze the impact of the maximum number of carriers allowed for CA user ( $\Delta_{\max}$ ) and the impact of the balancing threshold among fill-rates ( $\Theta_{\max}$ ) on the overall system performance. A system of 8 beams, 2 component carriers per beams and 120 users is considered. Fig. 9 depicts the impact of  $\Delta_{\max}$  on the overall capacity of a CA system. Note that  $\Delta_{\max} = 1$  defines a non-CA satellite system. Note that there is a decrease in the offered capacity when  $\Delta_{\max}$  increases from 1 to 2, i.e., the non-CA system has an overall higher offered capacity. However, it is important to note that in a non-CA system, the users cannot aggregate carriers, and the users associated with a given beam are served over the carriers primarily linked to the given beam. Typically, the users

get higher capacity when they are served by their own beams because of relatively higher SNRs compared to when they are served by neighboring beams. Therefore, in a non-CA system, although the overall offered capacity is higher, the amount of unmet/unused capacity is also higher. On the other hand, in a CA-based satellite system, although the offered capacity is slightly lower than the non-CA system, the peak rate of the users is improved, the fairness among the users in the system can be established, and more importantly, the amount of unmet as well as unused capacity is reduced. The most important feature to note is that allowing users to aggregate more than two component carriers does not add significant gain to the system performance. The offered capacity remains almost flat with varying  $\Delta_{\max}$ . In Fig. 9, we analyze the impact of  $\Theta_{\max}$  on the offered capacity. Favorably, the offered capacity is not affected much as the value of  $\Theta_{\max}$  is increased. The proposed CA solution is flexible enough to offer similar performance even when the imposed fill-rate constraint ( $\Theta_{\max}$ ) is tight.

Fig. 10 evaluates the Jain's Fairness Index as defined in (14) for different values of  $\Theta_{\max}$ . The results consider a system

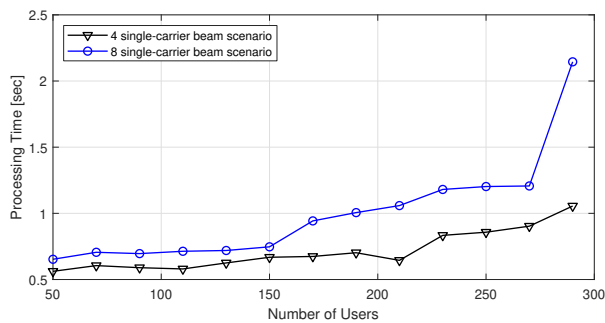


Fig. 11. Processing time of the proposed solution versus number of users in the system ( $N_U$ ).  $\Delta_{\max} = 4$ ,  $\Theta_{\max} = 0.20$ .

composed of 2 beams, 2 component carriers per beams and 25 users. The value of  $\Delta_{\max}$  is set to 4. For each value of  $\Theta_{\max}$ , 200 different demand realizations are shown. The results reveal that the proposed CA solution is extremely fair in all situations and the Jain's fairness index is very satisfactory. For lower values of  $\Theta_{\max}$ , the Jain's fairness index remains very stable over different demand realizations. For higher values of  $\Theta_{\max}$ , although the fairness index fluctuates slightly (the individual  $J_{FI}$ s for a small number of demand realizations may sometimes degrade, and in some cases, the  $J_{FI}$  with  $\Theta_{\max} = 0.50$  may go down as low as 0.984), but within a very limited extent and the overall fairness index remains very high. Therefore, we can conclude that lower values of  $\Theta_{\max}$  provide more flexibility to better match the demands in a fair manner. However, as the flexibility is restricted with higher values of  $\Theta_{\max}$ , the overall fair demand-matching performance degrades.

In order to assess the complexity of the proposed solution, we make use of the MATLAB function "timit", which measures the time required to run a function by running it several times and providing the average processing time. The experiments were carried out in an Intel(R) Core(TM) i5-8250U CPU @1.60 GHz. Assuming a scenario with a single-carrier per beam, Fig. 11 shows the impact of increasing the overall number of users in the processing time for two different scenarios with 4 and 8 beams. Clearly, the processing time increases with the number of users, but remaining slightly above 1 second for approximately 300 users for the 4 beam scenario, while surpassing 2 seconds for the 8 beam scenario. Although the numbers may scale rapidly for more beams and more users, we can expect the processing time to be of the order of seconds for a real system. This does not represent a threat for the forthcoming satellite systems which will be equipped with powerful processing units with cloud/edge computing capabilities [26].

## VI. CONCLUSIONS AND FUTURE WORKS

This paper studies the CA scheme in high throughput satellite systems. Different CA architectures and deployment scenarios have been presented, along with their advantages, disadvantages as well as technical challenges. In addition, an efficient multiuser aggregation and access control solution for CA have been proposed, in which the optimal carrier fill-rates and user-carrier assignment are derived. The performance

analysis of the proposed solution shows that CA can be very useful in enhancing the peak data rate of satellite users as well as in efficiently utilizing the available resources.

Although CA in satellite systems needs to be addressed at different levels of the communication stack, we have limited our focus only to system-level simulations with a PHY layer abstraction. The future study will take the impact of RF issues, for example, the impact of spectrum emission mask, adjacent carrier leakage ratio, non-linear satellite channel, etc., under consideration. Furthermore, the CA in this study is limited to GEO satellites, in particular, a single-satellite scenario. The feasibility and performance evaluation of CA in inter-satellite scenario [27] as well as in other orbitals, i.e., low earth orbit (LEO), MEO satellite systems are open research areas.

## ACKNOWLEDGMENT

The authors would like to thank Dr. Stefano Andrenacci and Dr. Joel Grotz from SES, and Nikolaos Toptsidis from ESA, for their support and valuable discussions and suggestions during the executions of this work.

## REFERENCES

- [1] M. G. Kibria, E. Lagunas, N. Maturo, D. Spano, H. Al-Hraishawi, and S. Chatzinotas, "Carrier Aggregation in Multi-Beam High Throughput Satellite Systems," in *2019 IEEE Global Communications Conference (GLOBECOM)*, 2019, pp. 1–6.
- [2] S. K. Sharma, S. Chatzinotas, and P.-D. Arapoglou, *Satellite Communications in the 5G Era*. IET Digital Library, 2018.
- [3] Y. Vasavada, R. Gopal, C. Ravishankar, G. Zakaria, and N. BenAmmar, "Architectures for next generation high throughput satellite systems," *International Journal of Satellite Communications and Networking*, vol. 34, no. 4, pp. 523–546, 2016. [Online]. Available: <https://onlinelibrary.wiley.com/doi/abs/10.1002/sat.1175>
- [4] O. Kodheli *et al.*, "Satellite Communications in the New Space Era: A Survey and Future Challenges," Feb. 2020, arXiv:2002.08811.
- [5] A. Paris, I. Del Portillo, B. Cameron, and E. Crawley, "A Genetic Algorithm for Joint Power and Bandwidth Allocation in Multibeam Satellite Systems," in *2019 IEEE Aerospace Conference*, March 2019, pp. 1–15.
- [6] G. Cocco, T. de Cola, M. Angelone, Z. Katona, and S. Erl, "Radio Resource Management Optimization of Flexible Satellite Payloads for DVB-S2 Systems," *IEEE Transactions on Broadcasting*, vol. 64, no. 2, pp. 266–280, Jun. 2018.
- [7] T. S. Abdu, E. Lagunas, S. Kisseleff, and S. Chatzinotas, "Carrier and Power Assignment for Flexible Broadband GEO Satellite Communications System," in *2020 IEEE International Symposium on Personal, Indoor and Mobile Radio Communications*, submitted paper.
- [8] C. N. Efrem and A. D. Panagopoulos, "Dynamic Energy-Efficient Power Allocation in Multibeam Satellite Systems," *IEEE Wireless Communications Letters*, vol. 9, no. 2, pp. 228–231, 2020.
- [9] J. J. Knab, "Optimum transponder gain and power for fully loaded satellite," *IEEE Transactions on Aerospace and Electronic Systems*, vol. 51, no. 4, pp. 3470–3474, 2015.
- [10] "TR 36.808, Evolved Universal Terrestrial Radio Access (E-UTRA); Carrier Aggregation; Base Station (BS) Radio Transmission and Reception," <https://portal.3gpp.org/>, accessed: 2020-06.
- [11] M. Iwamura, K. Etemad, M. Fong, R. Nory, and R. Love, "Carrier aggregation framework in 3GPP LTE-advanced [WiMAX/LTE Update]," *IEEE Communications Magazine*, vol. 48, no. 8, pp. 60–67, 2010.
- [12] H. S. Kamath, H. Singh, and A. Khanna, "Carrier Aggregation in LTE," in *2020 4th International Conference on Intelligent Computing and Control Systems (ICICCS)*, 2020, pp. 135–138.
- [13] H. Lee, S. Vahid, and K. Moessner, "A survey of radio resource management for spectrum aggregation in lte-advanced," *IEEE Communications Surveys Tutorials*, vol. 16, no. 2, pp. 745–760, 2014.
- [14] S. Kim, "Two-Level Game Based Spectrum Allocation Scheme for Multi-Flow Carrier Aggregation Technique," *IEEE Access*, vol. 8, pp. 89 291–89 299, 2020.



- [15] "ESA CADSAT Project: Carrier Aggregation in Satellite Communication Networks," <https://artes.esa.int/projects/cadsat>, accessed: 2020-06.
- [16] "Digital Video Broadcasting (DVB). (2014). DVB-S2X Standard [Online]," <https://www.dvb.org/standards/dvb-s2x>, accessed: 2020-06.
- [17] "NEWTEC chipsets supporting Channel Bonding," <https://www.newtec.eu/technology/channel-bonding>, accessed: 2020-06.
- [18] Z. Khan, H. Ahmadi, E. Hossain, M. Coupechoux, L. A. Dasilva, and J. J. Lehtomäki, "Carrier Aggregation/Channel Bonding in Next Generation Cellular Networks: Methods and Challenges," *IEEE Network*, vol. 28, no. 6, pp. 34–40, 2014.
- [19] H. Al-Hraishawi, N. Maturo, E. Lagunas, and S. Chatzinotas, "Perceptive Packet Scheduling for Carrier Aggregation in Satellite Communication Systems," in *IEEE Int. Conf on Commun. (ICC), Dublin, Ireland*, Jun. 2020, pp. 1–6.
- [20] "SES ASTRA: GEO satellite family devoted to broadcasting system," <https://astra.ses/>, accessed: 2020-06.
- [21] G. Taricco and A. Ginesi, "Precoding for flexible high throughput satellites: Hot-spot scenario," *IEEE Transactions on Broadcasting*, vol. 65, no. 1, pp. 65–72, 2019.
- [22] "SES Medium Earth Orbit (MEO) constellation O3b mPOWER [Online]," <https://www.ses.com/networks/networks-and-platforms/o3b-mpower>, accessed: 2020-06.
- [23] M. Grant and S. Boyd, "CVX: Matlab software for disciplined convex programming, version 2.1," <http://cvxr.com/cvx>, Mar. 2014.
- [24] R. Jain, D. Chiu, and W. Hawe, "A Quantitative Measure of Fairness and Discrimination for Resource Allocation in Shared Computer System," *DEC Technical Report 301*, 1984.
- [25] "Carrier Aggregation in Satellite Communication Networks (CADSAT) SW Tool 2," [https://www.fir.uni.lu/snt/research/sigcom/sw\\_simulators/cadsat](https://www.fir.uni.lu/snt/research/sigcom/sw_simulators/cadsat), accessed: 2020-06.
- [26] NetWorld 2020, Satellite Communications Working Group, "SatCom Resources for Smart and Sustainable Networks and Services," *White Paper*, pp. 1–26, 2019. [Online]. Available: [https://www.networld2020.eu/wp-content/uploads/2019/11/satcom-ss-whitepaper\\_v1\\_final.pdf](https://www.networld2020.eu/wp-content/uploads/2019/11/satcom-ss-whitepaper_v1_final.pdf)
- [27] R. Radhakrishnan, W. W. Edmonson, F. Afghah, R. M. Rodriguez-Osorio, F. Pinto, and S. C. Burleigh, "Survey of inter-satellite communication for small satellite systems: Physical layer to network layer view," *IEEE Communications Surveys Tutorials*, vol. 18, no. 4, pp. 2442–2473, 2016.

**Mirza Golam Kibria** (Member, IEEE) received the B.E. degree from Visveswaraiya Technological University (VTU), India, in 2005, the M.Sc. degree from the Lund Institute of Technology (LTH), Lund University, Sweden, in 2010, and the Ph.D. degree from Kyoto University, Japan, in 2014, all in electrical engineering. He was with the Wireless Network Research Center, National Institute of Information and Communications Technology (NICT), Yokosuka Research Park, Japan, from July 2014 to August 2018, and with University of Luxembourg between 2018 and 2020. He is currently working at HUAWEI R&D Sweden. His research interests include satellite communications, resource allocation optimization, wireless signal processing, small cell networks, and stochastic geometry. He was an awardee of Japanese Government Scholarship. He was a recipient of the Young Researcher's Encouragement Award from the Japan chapter of the IEEE Vehicular Technology Society (VTS), in 2012, the IEICEWBS Student Paper Award, in 2013, and the IEEE WPMC Best Paper Award, in 2015.

**Eva Lagunas** (S'09-M'13-SM'18) received the MSc and PhD degrees in telecommunications engineering from the Polytechnic University of Catalonia (UPC), Barcelona, Spain, in 2010 and 2014, respectively. She was Research Assistant within the Department of Signal Theory and Communications, UPC, from 2009 to 2013. In 2009 she was a guest research assistant within the Department of Information Engineering, University of Pisa, Italy. From November 2011 to May 2012 she held a visiting research appointment at the Center for Advanced Communications (CAC), Villanova University, PA, USA. In 2014, she joined the Interdisciplinary Centre for Security, Reliability and Trust (SnT), University of Luxembourg, where she currently holds a Research Scientist position. Her research interests include radio resource management and general wireless networks optimization.

**Nicola Maturo** (M'13) received his M.S. Degree in Electronic Engineering (cum laude) from the Polytechnic University of Marche, Ancona (Italy), in 2012 and his Ph.D. on Telecommunication Engineering in the same University, in 2015. From January 2016 to July 2017 he was a Post-Doctoral Researcher at the Department of Information Engineering of the Polytechnic University of Marche, where he worked on error correcting coding techniques under some ESA research projects. From November 2015 to May 2016 he was consultant for Deimos Engenharia (Lisbon) working on spectral estimation algorithms and anti-jamming techniques. Since August 2017 he is a Research Associate at the University of Luxembourg. His research activity is mainly focused on the development and implementation of advanced techniques for satellite communication. He is a member of IEEE since 2013 and of the CCSDS Coding and Synchronization Working Groups since 2015.

**Hayder Al-Hraishawi** received the B.Sc. and M.Sc. degrees (First Class Hons.) in electrical engineering from the Department of Electrical Engineering, Al-Mustansiriyah University, Baghdad, Iraq, in 2003 and 2006, respectively, and the Ph.D. degree from the Department of Electrical and Computer Engineering, Southern Illinois University Carbondale, USA, in 2017. In 2018, he joined the University of Luxembourg, where he currently holds a research associate position. His current research interests include design and analysis of spectrum-sharing techniques for massive MIMO systems, resource management for satellite communications and wireless energy harvesting.

**Symeon Chatzinotas** (S'06-M'09-SM'13) is currently Full Professor / Chief Scientist I and Co-Head of the SIGCOM Research Group at SnT, University of Luxembourg. In the past, he has been a Visiting Professor at the University of Parma, Italy and he was involved in numerous Research and Development projects for the National Center for Scientific Research Demokritos, the Center of Research and Technology Hellas and the Center of Communication Systems Research, University of Surrey. He received the M.Eng. degree in telecommunications from the Aristotle University of Thessaloniki, Thessaloniki, Greece, in 2003, and the M.Sc. and Ph.D. degrees in electronic engineering from the University of Surrey, Surrey, U.K., in 2006 and 2009, respectively. He was a co-recipient of the 2014 IEEE Distinguished Contributions to Satellite Communications Award, the CROWNCOM 2015 Best Paper Award and the 2018 EURASIP JWCN Best Paper Award. He has (co-)authored more than 400 technical papers in refereed international journals, conferences and scientific books. He is currently in the editorial board of the IEEE Open Journal of Vehicular Technology and the International Journal of Satellite Communications and Networking.